



MIT Open Access Articles

Filling the terahertz gap with sand: High-power terahertz radiators in silicon

The MIT Faculty has made this article openly available. **Please share** how this access benefits you. Your story matters.

Citation	Han, Ruonan and Afshari, Ehsan. 2015. "Filling the terahertz gap with sand: High-power terahertz radiators in silicon."
As Published	10.1109/bctm.2015.7340574
Publisher	IEEE
Version	Author's final manuscript
Citable link	https://hdl.handle.net/1721.1/137638
Terms of Use	Creative Commons Attribution-Noncommercial-Share Alike
Detailed Terms	http://creativecommons.org/licenses/by-nc-sa/4.0/

Filling the Terahertz Gap with Sand: High-Power Terahertz Radiators in Silicon

(Invited Paper)

Ruonan Han^{1,2} and Ehsan Afshari¹

¹Cornell University, Ithaca, NY, 14850, USA

²Massachusetts Institute of Technology, Cambridge, MA, 02139, USA

Abstract—This paper reviews our recent work on Si and SiGe THz sources that generate high-power coherent radiation. Our design approach blends the optimization of device operation near or above f_{max} with unconventional circuit topologies and energy-efficient electromagnetic structures. Using a 130-nm SiGe HBT process (f_{max} =280 GHz), our 320-GHz transmitter produces a record radiated power (3.3 mW) and DC-to-THz radiation efficiency (0.54%) among all THz signal sources in silicon. This transmitter also demonstrates fully-integrated phase-locking capability for THz radiators for the first time. In this paper, a 260-GHz pulse radiator and a 340-GHz phased array, which are based on a 65-nm bulk CMOS process, are also presented. The former generates a radiated power of 1.1 mW, and provides THz pulses with 25-GHz bandwidth. The latter generates a radiated power of 0.8 mW and has a 50° beam-steering capability. These works demonstrate a promising roadmap towards future THz microsystems using silicon integrated-circuit technologies.

I. INTRODUCTION

The monolithic implementation of terahertz (THz) systems on low-cost silicon chips is a very promising solution to open up wide applications of THz radiation in the areas of medical care, industrial product inspections, and security screening [1],[2]. It is expected that these chips will enable affordable and portable products such as *in-vivo* tooth cavity detection [3], breath analyzer for disease diagnosis [4] and handheld scanner for contrabands and explosives [5]. However, building on-chip THz components and systems, especially radiation sources, are challenging and requires a totally different design approach from that in the RF (and also low mm-Wave) frequencies. Conventionally, circuit designers has been exploiting the ever increasing speed of devices, which is enabled by the scaling of the silicon integrated technologies. Without much modification to the circuit topologies, existing designs could often be applied to higher frequencies with smaller sizes and values of the components (capacitor, inductor, transistor, etc.)—as long as the operation frequency is a small fraction ($<1/3$) of the f_{max} of the device. Unfortunately, the growth of the f_{max} in the mainstream CMOS/BiCMOS technologies has slowed down in the recent years. So as we aggressively enter the terahertz regime, the following issues have emerged.

First, the fundamental operation frequency f_0 is so close to the cut-off frequency of the device ($f_0 > f_{max}/2$) that the active gain of the device becomes very small. Meanwhile,

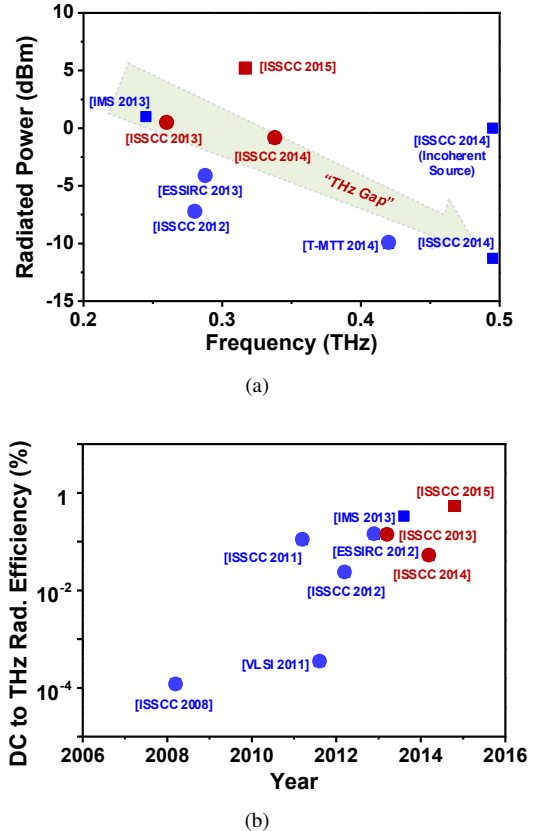


Fig. 1. State-of-the-art THz sources implemented using CMOS transistors (round dots) and SiGe HBT (square dots) (a) the total radiated power, and (b) DC-to-THz radiation efficiency. The dots in red are the works described in this paper.

the breakdown voltage of the highly-scaled silicon transistors keeps decreasing, which severely limits the power handling capabilities of these devices. Such scarce device efficacy is further reduced by the larger loss of the on-chip metal structures due to the deteriorating skin-depth effect and the doped silicon substrate. The latter is especially detrimental to the on-chip radiation, due to the substrate-mode excitation.

Second, since the target output frequency is normally above the f_{max} , we have to rely on harmonic generations. In fact, the ubiquitous usage of device nonlinearities and harmonic

generation is probably the biggest distinction between THz electronics and its lower-frequency counterparts. While the modeling and optimization of the nonlinearity in two-terminal devices, such as diodes and varactors, were well studied [6],[7], those for the three-terminal transistors remain unsolved. This greatly adds the complexity of the design. It is noteworthy that the harmonic operation also inevitably leads to lower energy efficiency.

Lastly, if the design of a THz source follows the traditional method involving multiple, single-function blocks (e.g. oscillation, harmonic generation, signal filtering and on-chip radiation), significant interconnect loss and bandwidth degradation will occur [8]. Such approach also increases the size of the radiation source, which lowers the power-generation density and leads to large radiation side lobes in an array configuration.

Due to these issues, the output power of the state-of-the-art silicon radiators is still at milli-watt level, which is plotted in Fig. 1(a). The generated power also drops quickly at a rate of $1/f_{out}^3$ to $1/f_{out}^4$. On the other hand, the DC-to-THz radiation efficiency is shown in Fig. 1(b). Currently, the absolute efficiency value is still below 1%; but fortunately, ever since the first CMOS THz radiator reported in 2008 [9], the efficiency has been improved by over 1000x. These plots also clearly show the advantages of SiGe heterojunction bipolar transistors (HBTs), which have higher f_{max} and breakdown voltage compared to the silicon MOSFETs [10].

In this paper, we introduce a device-centric design approach. Through analyses that are independent of any specific design topology, the limit of harmonic generation from a single transistor are first examined. Then, the conditions associated with the device limits are utilized as the guidelines and requirements for the synthesis of unconventional THz circuits. As a result of such “bottom-up” design methodology, the small device efficacy at THz is fully exploited. In addition, our approach also blends the device optimizations with the electromagnetic design, in order to minimize the circuit loss and footprint.

Next, several THz radiator prototypes are reviewed, which illustrate our coherent efforts from the investigation of a single-device operation to the creation of novel, scalable architectures. These works not only represent the highest radiated power and energy efficiency among all THz sources in silicon [11] (Fig. 1), but also demonstrate various critical functionalities for future THz microsystems, such as phase locking [11], short-pulse generation [12] and beam steering [13].

II. 320-GHZ TRANSMITTER WITH INTEGRATED PHASE LOCKING

This 320-GHz transmitter consisting of 16 mutually-coupled radiator array [11]. It is implemented using a 130-nm SiGe:C BiCMOS process ($f_T/f_{max}=220/280$ GHz) from STMicroelectronics. Through free-space power combining, the transmitter achieves a radiated power of 3.3 mW and DC-to-THz radiation efficiency of 0.54% (Fig. 2(a)). It is noteworthy that the chip is also equipped with a phase-locked loop, which is critical for heterodyne imaging with enhanced sensitivity and

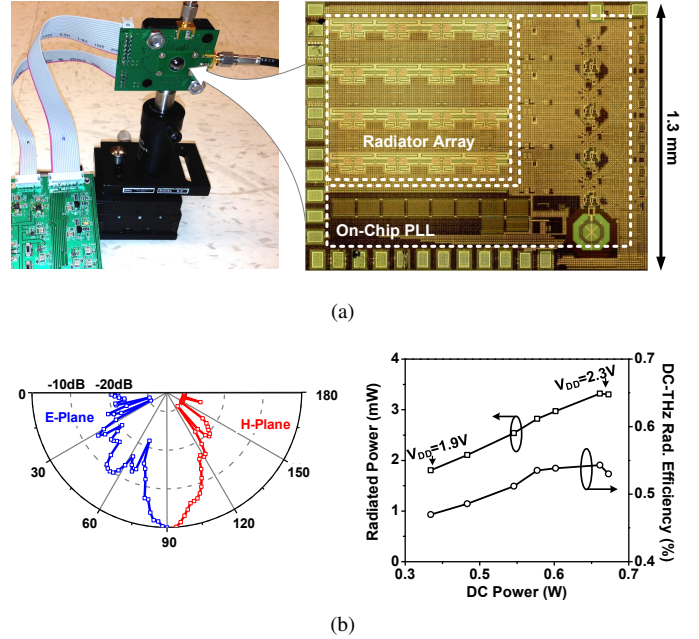


Fig. 2. (a) The die photo and package of the 320-GHz transmitter. (b) Measured radiation pattern, power, and DC-to-THz radiation efficiency.

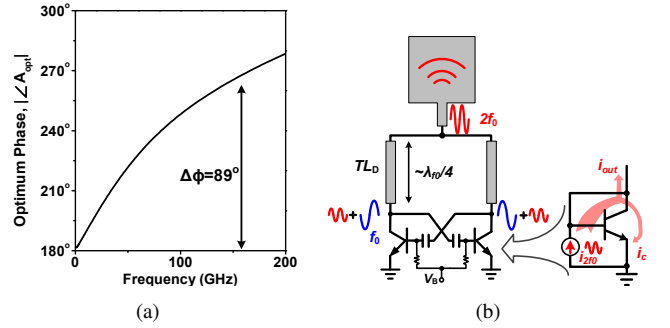


Fig. 3. (a) The simulated phase of the optimum gain of a 130-nm SiGe HBT. (b) The equivalent diode-connected configuration of a transistor inside a push-push oscillator at $2f_0$ due to the unity harmonic feedback factor ($\beta_{2f_0}=1$).

beam forming capabilities. To our best knowledge, this is the first demonstration of fully-integrated phase locking in THz radiators¹.

The key component of this work, the THz radiator, is based on harmonic oscillator, which is normally more efficient than frequency multipliers due to its self-sustaining nature. The design target of the radiator is to optimize the following three steps of the signal generation².

- 1) At the fundamental frequency f_0 , the transistor should be configured to generate the maximum power, in order to overcome the passive loss and sustain a large oscillation swing. It is found that an optimum complex voltage gain A_{opt} is required to achieve this [15]. To be more specific, both the device analyses and mathematical derivations have indicated that, as the oscillation

¹The first THz phased-locked loop in silicon is demonstrated in [14]. In this work, the output power is measured through on-wafer probing.

²It is noteworthy that these analyses theories are applicable for both SiGe HBTs and CMOS transistors.

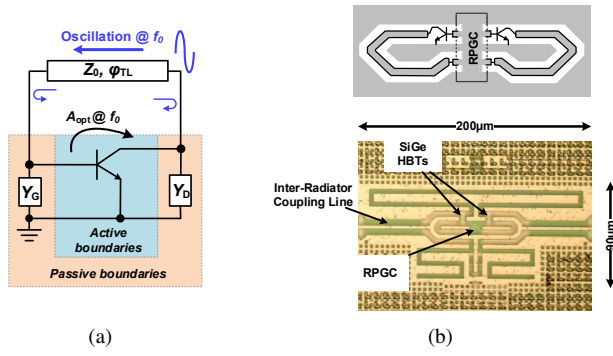


Fig. 4. (a) A simplified schematic of the proposed self-feeding oscillator structure. (b) The proposed THz radiator design based on a differential self-feeding oscillator pair and a return-path gap coupler.

frequency approaches f_{max} , the phase delay of A_{opt} is significantly larger than 180° (i.e. full inversion operation) (Fig. 3(a)). Intuitively, such required extra phase shift is for matching the delay of the device transconductance (input voltage to output current). This delay is caused by the finite carrier transit time and gate/base-to-drain/collector feedforward current through the parasitic capacitance (e.g. C_μ in HBTs). Unfortunately, in the commonly-used push-push oscillators, the phase of the transistor gain is forced to be 180° , which leads to under-optimized oscillation power.

- 2) The nonlinearity of the device needs to be fully utilized so as to efficiently convert the fundamental power into higher harmonic (e.g. $2f_0$). It is noteworthy that simply performing impedance matching at the output is not sufficient [16]. We found that such nonlinear process is strongly related to the harmonic feedback factor β_{2f_0} between the two device terminals through the peripheral oscillator structure. Unfortunately, such feedback is negative in many conventional designs, and reduces the net output power. For example, in a push-push oscillator, the 2nd-harmonic voltages at both terminals of a transistor are identical (Fig. 3(b)). Through such unity harmonic feedback factor ($\beta_{2f_0}=1$), an additional harmonic current is induced at the collector, which partially cancels the current originally generated through the f_0 -to- $2f_0$ up conversion from the base. This partly explains the low power levels of the sources reported previously. In THz range, the optimum β_{2f_0} is close to zero, which means effective harmonic isolation is required.
- 3) It is desired that the generated harmonic signal be directly radiated with minimum power loss in the antenna feed lines. This is unfortunately not the case in conventional designs. In the multi-push topologies (Fig. 3(b)), the harmonic signal needs to travel along the resonators used for oscillation at f_0 before reaching the antenna. The length of the resonator at harmonic frequencies is close to $\lambda/2$ (push-push) and $3\lambda/4$ (triple-push), which leads to significant power loss.

To meet the first condition, a “self-feeding” oscillator topology is adopted in our radiator design. The basic schematic

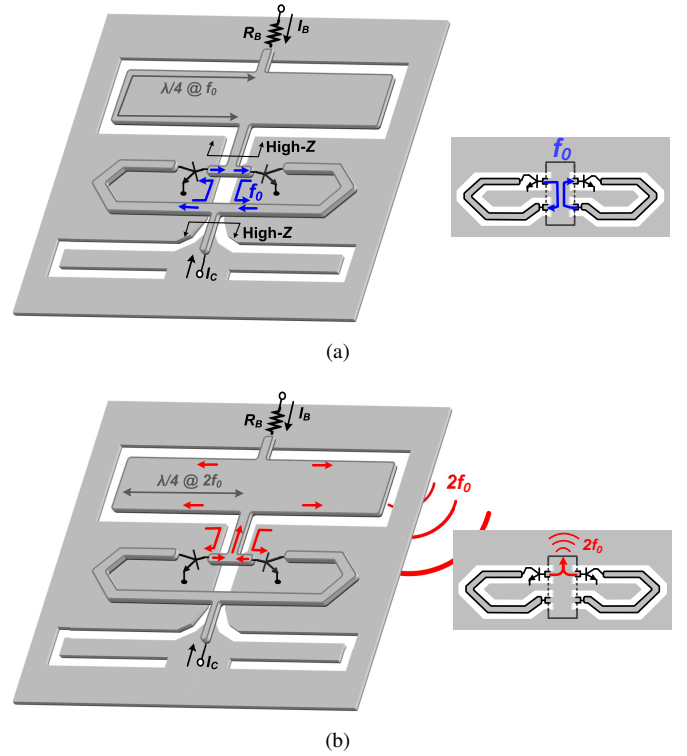


Fig. 5. (a) A simplified schematic of the proposed self-feeding oscillator structure. (b) The proposed THz radiator design based on a differential self-feeding oscillator pair and a return-path gap coupler.

is shown in Fig. 4(a), where a transmission line (TL) is used as the oscillation feedback path. The transistor, as well as the admittances Y_G and Y_D are treated as the boundary conditions for the wave propagation and reflection inside the TL. Using linear network theories, we show that when the design parameters in Fig. 4(a) comply with the following relationship:

$$\frac{1}{Z_0 \sin \varphi_{TL}} = \frac{g_{11} + \text{Re}(A_{opt} \cdot y_{12})}{\text{Im}(A_{opt})}, \quad (1)$$

A_{opt} can be achieved [16]. In (1), Z_0 and φ_{TL} are the impedance and electrical length of the transmission line, and g_{11} and y_{12} are the Y-parameters of the transistor.

Next, to achieve the effective harmonic isolation, a return-path gap coupler (RPGC) structure is inserted into the feedback paths of a differential self-feeding oscillator pair (Fig. 4(b) and Fig. 5). The RPGC, essentially a two-conductor waveguide, allows the propagation of an odd-mode signal. Therefore, as Fig. 5(a) shows, the return currents of the differential oscillation signals from the collectors can pass the RPGC with very small delay and insertion loss (0.6 dB in simulation). Once they arrive at the other side of the RPGC, forward currents are induced inside the microstrip transmission lines and injected into the bases of the HBTs. In Fig. 5(a), the two slot pairs at the top and bottom of the RPGC behave as quarter-wave transformers, which present high impedance to the oscillation signal, so as to confine the odd-mode wave in the center of the RPGC.

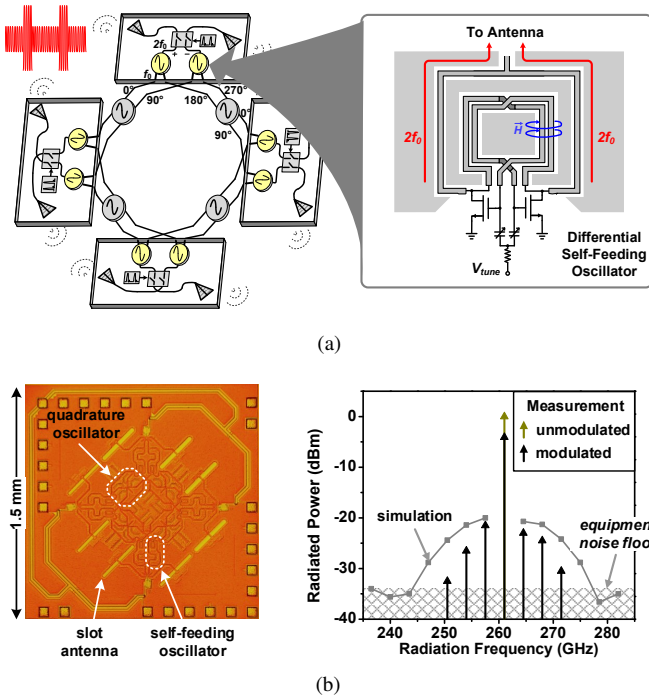


Fig. 6. 260-GHz pulse radiator array: (a) architecture, (b) the die photo and the measured radiated spectrums.

On the other hand, the up-converted 2^{nd} -harmonic signal³ is in even mode. Since the return-path gap does not support the propagation of even-mode wave⁴, the harmonic signal is fully blocked (Fig. 5(b)), and effective isolation at $2f_0$ is achieved (>35 dB in simulation). Interestingly, the slot pair at the top, which is used as wave chokes at f_0 , now behaves as a typical folded-slot antenna in which four quarter-wave sections radiate in phase. This not only eliminates the need for any explicit antenna structure, but also ensures that the harmonic signal is radiated right after its generation from the devices.

It can be seen that by utilizing wave formation, propagation, and mode orthogonality, our radiator structure simultaneously optimizes fundamental oscillation, harmonic generation, and on-chip radiation. Due to its compactness, the area of the 4×4 radiator array is only 0.8 mm^2 .

Since the THz wave is exposed to the substrate through the slots, the generated radiation is absorbed into the silicon. To eliminate the excitation of the substrate wave and couple the radiation into free space, a high resistivity hemispheric silicon lens is attached to the chip back, which leads to $\sim 40\%$ radiation efficiency in the simulation. Nevertheless, even without the lens, the measured total power of the direct backside radiation is still as high as 1.2 mW . The small degradation is due to the high density of the in-phase radiators: the divergence of the near-field radiated wave is suppressed by the vertical high-impedance boundaries created by neighboring radiators. The excitation of substrate wave, as well as the reflection loss at the silicon-to-air interface, are therefore minimized.

³In this work, the harmonic signal at $2f_0$ is extracted from the base heterojunctions of the HBTs.

⁴The cutoff frequency for this mode in the two-conductor waveguide is $\sim 6 \text{ THz}$.

III. 260-GHz CMOS RADIATOR WITH NARROW-PULSE MODULATION

It is noteworthy that the proposed device-centric THz design approach is applicable to other processes (CMOS, III-V compound semiconductors, etc.). As one example, the self-feeding oscillator with maximum oscillation activity is also implemented in a 260-GHz CMOS pulse radiator array [12].

The architecture of this signal source is shown in Fig. 6(a), which consists of a loop of four differential radiator blocks. Each radiator block contains one pair of differential self-feeding oscillators. Different from the 320-GHz transmitter in Section II, the differential operation of the self-feeding oscillator in this work is realized through the magnetic coupling of the self-feeding lines. Next, neighboring oscillator pairs are coupled with quadrature phase, so that their 2^{nd} -harmonic outputs are out-of-phase. This facilitates the layout and placement of the slot antennas for backside radiation.

It is noteworthy that in (1), Z_0 and φ_{TL} are coupled and provide some freedom in choosing their values. Such flexibility is utilized for the harmonic isolation between the MOSFET terminals: the length of the self-feeding transmission line at $2f_0$ is chosen to be near quarter-wave ($\varphi_{TL, f_0} = 48^\circ$). The line then transforms the low impedance at gate (due to large C_{gs}) into a much higher one presented at the drain side. The high impedance therefore keeps the generated harmonic signal from flowing back to the gate. In our simulation, such isolation increases the harmonic generation efficiency by 4 times.

This signal source is implemented using TSMC 65-nm bulk CMOS process (Fig. 6(b)). In the measurement, the total radiated power is 1.1 mW , which is so far the highest among all CMOS radiators operating in this frequency range. On this chip, varactor-based switches are also integrated, in order to modulate the radiation with very narrow pulses ($\tau \approx 45 \text{ pS}$) generated on chip. Under such modulation, the measured spectrum of the output beam fully covers a 25-GHz bandwidth. This demonstrates its potential applications in terahertz spectroscopy.

IV. 340-GHz PHASED ARRAY: A HIGHLY-SCALABLE ARCHITECTURE

For power generation at terahertz, an array of small radiators is normally more efficient than increasing the power of a single source. In addition, the spatial diversity of a distributed source has the ability to focus the beam at the desired point in space. In other words, by splitting a single source into N smaller elements with the same total DC power, the effective radiated power targeted at a certain point can increase by a factor of N . Nevertheless, the main challenge with scaling is to maintain control over the individual elements in the same way that one accesses a single module. In fact, this challenge has shaped the conventional idea for phased array radiation. As shown in Fig. 7(a), the control of the multiple sources in a phased array is through a single source that distributes its power across the grid through a global network. The complexity of this global routing becomes noticeable as the number of rows and columns in the array increases and/or the interconnect coupling and loss start to affect the performance. In order to

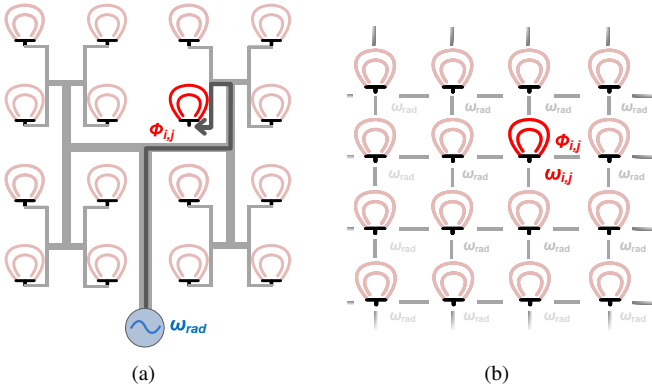


Fig. 7. (a) The conventional implementation of the phased array concept. (b) An ideal scalable phased array radiator with local coupling between adjacent cores.

build a scalable source that can steadily increase the limited performance of individual devices without mounting structural complexity, a 2-D scalable and tunable THz source based on delay-coupled oscillators is presented [13].

The concept of the scalable phased array is based on the local, mutual interactions between radiator units. Shown in Fig. 7(b), these independent terahertz radiators are separated from their neighbors by half the wavelength. In this arrangement, instead of using a single control unit, the oscillators synchronize to each other as a result of the local coupling between adjacent neighbors. There is no lengthy, global interconnects, and with the absence of uncertainties due to error and loss propagation, the scaling of the structure is not bound to a small number of elements.

Interestingly, the method to adjust the phase and frequency of this structure proves to be quite intuitive. In a ring of oscillators that are directionally coupled by phase shifters, we show that the synchronized frequency can be controlled by adjusting the coupler phase shifts [17]. We call this common phase shift ϕ_c that is changed across all couplers. In the 2-D array, the same adjustment to the common phase shift will change the synchronized frequency of the radiators. As shown in Fig. 8(a), we can illustrate the coupling phase shifts of the network by a bundle of phasors in the array phase space. The common phase shift is in effect a superposition of all the phasors. When all the phasors are aligned, the radiators are in phase. Now, if the phase shift of the couplers surrounding one of the radiators change in opposite directions, ϕ_c remains unchanged. However, the phase of that particular node changes according to this differential change, ϕ_d . We demonstrate that a particular mapping exists between all possible changes in the ϕ_d 's and all the angles of the radiated beam of the phase array. This 2-D phased array concept based on the theory of coupled oscillator provides a method to independently control the phase and frequency properties of a scalable structure in a fully distributed fashion. This offers a suitable solution for a terahertz source that can be scaled without the limitations of previous controlling methods.

To prove the concept, a 4×4 phased array at 340 GHz is implemented using a 65-nm CMOS process [13]. The signal is radiated through on-chip patch antennas to the front side.

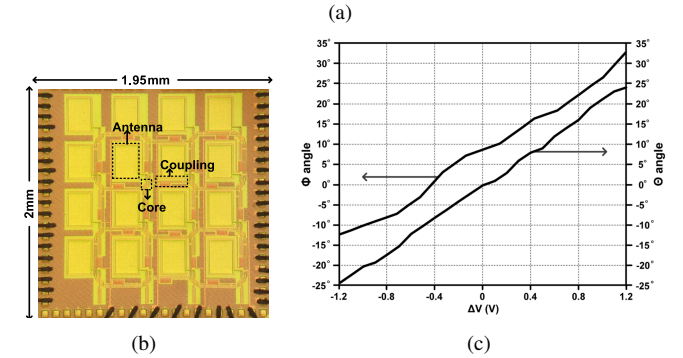
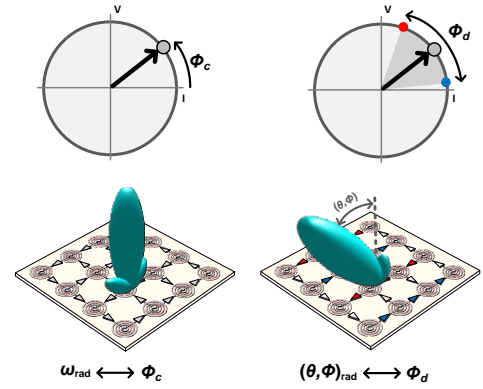


Fig. 8. (a) Left: frequency tuning of the phased array by changing the common phase. Right: Phase tuning and beam steering in the array by performing differential phase adjustments. (b) Die photos of a 340-GHz tunable phased array radiator based on delay-coupled oscillators. (c)

Without any post processing and silicon lens coupling, the measured radiated power is 0.8 mW. This chip demonstrates the first fully integrated beam steering above 300 GHz with a measured maximum steering angle of $\sim 50^\circ$ in the 2D space (Fig. 8(c)).

V. CONCLUSION

The performance and capabilities demonstrated by our chips have shown great potential of standard SiGe BiCMOS and Si CMOS processes in implementing future THz microsystems. With the scaling of the devices, especially the near half-THz f_{max} that SiGe HBTs exhibit recently [10], such potential should be able to soon turn into THz components and systems with even higher performance and complexity. We expect that these progress will eventually trigger the wide applications of the THz spectrum.

VI. ACKNOWLEDGEMENT

The work presented in this paper are supported by the National Science Foundation (NSF), Army Research Lab (ARL), and C2S2 Focus Center under the Focus Center Research Program (FCRP), a Semiconductor Research Corporation (SRC) entity. We acknowledge the STMicroelectronics and the TSMC University Shuttle Program for the chip fabrications. We are also thankful for the previous and current members of the Ultra-Nonlinear-High-Speed IC Lab (UNIC) at Cornell University, who are involved in these THz projects: Prof.

Omeed Momeni (now with UC Davis), Dr. Yahya Tousi (now with IBM), and Dr. Muhammad Adnan (now with MediaTek), Chen Jiang, Ali Mostajeran and Hamidreza Aghasi.

REFERENCES

- [1] M. Tonouchi, "Cutting-edge terahertz technology," *Nature Photonics*, vol. 1, no. 2, pp. 97–105, Feb. 2007.
- [2] E. Seok, D. Shim, C. Mao, R. Han, S. Sankaran, C. Cao, W. Knap, and K. K. O, "Progress and challenges towards terahertz cmos integrated circuits," *IEEE J. Solid-State Circuits*, vol. 45, no. 8, pp. 1554–1564, Aug. 2010.
- [3] E. Pickwell and V. Wallace, "Biomedical applications of terahertz technology," *Journal of Physics D: Applied Physics*, vol. 39, pp. R301–R310, Aug. 2006.
- [4] A. Fosnight, B. Moran, and I. Medvedev, "Chemical analysis of exhaled human breath using a terahertz spectroscopic approach," *Applied Physics Letters*, vol. 103, no. 13, 2013.
- [5] W. Spiegel, M. Bauer, M. Fanzhen, M. Thomson, S. Boppel, A. Lisauskas, B. Hils, V. Krozer, A. Keil, T. Loffler, R. Henneberger, A. Huhn, G. Spickermann, P. Bolivar and H. Roskos, "Thz active imaging systems with real-time capabilities," *IEEE Trans. on Terahertz Science and Technology*, vol. 1, no. 1, pp. 183–200, Sep. 2011.
- [6] P. Penfield and R. Rafuse, *Varactor Applications*, M.I.T. Technology Press, Cambridge, MA, 1962.
- [7] R. Han and E. Afshari, "A high-power broadband passive terahertz frequency doubler in CMOS," *IEEE Trans. Microw. Theory Tech.*, vol. 61, no. 3, pp. 1150–1160, Mar. 2013.
- [8] A. Hajimiri, "The future of high frequency circuit design," in *Proc. European Solid-State Circuits Conf. (ESSIRC)*, Sep. 2009.
- [9] E. Seok, C. Cao, D. Shim, D.J. Arenas, D.B. Tanner, C.M. Hung and K.K.O, "A 410GHz CMOS Push-Push oscillator with an on-chip patch antenna," in *Intl. Solid-State Circuits Conf. (ISSCC)*, San Francisco, CA, Feb. 2008.
- [10] R. L. Schmid, A. Ulusoy, S. Zeinolabedinzadeh, and J. D. Cressler, "A comparison of the degradation in RF performance due to device interconnects in advanced SiGe HBT and CMOS technologies," *IEEE Trans. Electron Devices*, vol. PP, no. 99, Apr. 2015.
- [11] R. Han, C. Jiang, A. Mostajeran, M. Emadi, H. Aghasi, H. Sherry, A. Cathelin, and E. Afshari, "A 320GHz transmitter with 3.3mW phase-locked radiation for heterodyne imaging systems," in *Intl. Solid-State Circuits Conf. (ISSCC)*, San Francisco, CA, Feb. 2015.
- [12] R. Han and E. Afshari, "A 260GHz broadband source with 1.1mW continuous-wave radiated power and EIRP of 15.7dBm in 65nm CMOS," in *Intl. Solid-State Circuits Conf. (ISSCC)*, San Francisco, CA, Feb. 2013.
- [13] Y. Tousi and E. Afshari, "A Scalable THz 2D phased array with +17dBm of EIRP at 338GHz in 65nm bulk CMOS," in *Intl. Solid-State Circuits Conf. (ISSCC)*, San Francisco, CA, Feb. 2014.
- [14] P. Y. Chiang, Z. Wang, O. Momeni, and P. Heydari, "A 300GHz frequency synthesizer with 7.9% locking range in 90nm SiGe BiCMOS," in *Intl. Solid-State Circuits Conf. (ISSCC)*, San Francisco, CA, Feb. 2014.
- [15] O. Momeni and E. Afshari, "High power terahertz and sub-millimeter wave oscillator design: a systematic approach," *IEEE J. Solid-State Circuits*, vol. 46, no. 3, pp. 583–597, Mar. 2011.
- [16] R. Han, E. Afshari, "A CMOS high-power broadband 260-GHz radiator array for spectroscopy," *IEEE J. Solid-State Circuits*, vol. 48, no. 12, pp. 3090–3104, Dec. 2013.
- [17] Y. Tousi and E. Afshari, "Delay coupled oscillators for frequency tuning of solid-state terahertz sources," *Physical Review Letters*, vol. 23, no. 108, Jun. 2012.